AERE - R 4597

INDSWG-59

INDC(UK)*008G

AERE - R 4597

UNCLASSIFIED

(Approved for Publication)

E·MINIMIS·MAXIMA

United Kingdom Atomic Energy Authority

RESEARCH GROUP

Report

A FISSION CROSS SECTION OF Pu^{241} FROM 0.01 eV TO 3 keV

G. D. JAMES

Nuclear Physics Division,

Atomic Energy Research Establishment,

Harwell, Berkshire.

1964

U.D.C.
546.799.4.02.241 :539.173.4
539.173.4

UNCLASSIFIED
Approved for Publication

AERE - R 4597

THE FISSION CROSS SECTION OF Pu^{241} FROM 0.01 eV TO 3 keV

By

G. D. James

ABSTRACT

The fission cross section of Pu^{241} has been measured from 0.01 eV to 3 keV by the time-of-flight method. Below 11 eV the data are in fair agreement with the cross section given by the multilevel parameters of Simpson and Moore. A multilevel analysis of the cross section from 11 eV to 17 eV has been carried out. The errors in the mean fission cross section are discussed.

Nuclear Physics Division,
U.K.A.E.A., Research Group,
Atomic Energy Research Establishment,
HARWELL.

May 1964.

HL 64/3931 (C17).
BEKW

CONTENTS

TABLES

ILLUSTRATIONS

1. INTRODUCTION

The fission cross section of the Pu^{241} nucleus as a function of neutron energy is required for the determination of the reactivity and Döppler coefficient of nuclear reactors containing highly irradiated fuel. Reactivity calculations require data that provide accurate average values of the cross section over wide neutron energy bands whereas a determination of the Döppler coefficient requires a knowledge of the resonance parameters to as high a neutron energy as possible. The cross section is also of interest because it adds to our knowledge of the relatively few nuclei which undergo fission by neutrons of thermal energy. It has been shown that these nuclei exhibit strong resonance-resonance interference due to the small number of fission channels which are available. Simpson and Moore(1) have shown that the interference effects observed in the total cross section of Pu^{241} below 11 eV can be adequately described using a multilevel formula developed by Reich and Moore(15). The measurements of the fission cross section by Watanabe and Simpson(2) indicate that the multilevel results of Simpson and Moore are substantially correct. More recently Moore et al(22) have measured the fission cross section from 2 eV to 100 eV and performed a multilevel analysis of the data below 36 eV. Several measurements of the fission cross section of Pu^{241} have been made(3,4,5) but only the measurements of Adamchuk et al(5) and Moore et al(22) extend beyond 20 eV.

This report describes a time-of-flight measurement of the fission cross section of Pu^{241} from 0.01 eV to 3 keV and discusses the accuracy of the mean value of the fission cross section over neutron energy (E) ranges E to 2E. The data below 11 eV are compared with the multilevel cross section given by Simpson and Moore. From 11 eV to 17 eV a multilevel analysis of the data has been carried out for an assumed constant value of the radiation width; the mean level spacing, the strength function and the distribution of fission widths for the resonances below 20 eV have been found.

2. EXPERIMENTAL METHOD

2.1 The time-of-flight equipment

The fission cross section of Pu^{241} has been measured on a time-of-flight spectrometer using the Harwell electron linear accelerator and neutron booster source. Two experiments were carried out, one using a 5m flight path covered the neutron energy range 0.0087 eV to 20 eV, the other covered the range 3 eV to 3 keV and used a 15m flight path. Figs 1 and 2 show the flight path layout for these two experiments and also a schematic diagram of the electronics. A part of the 15m flight path was evacuated. Signals from the fission chambers which contained the surface barrier detectors described in §2.2, were sent through a pre-amplifier to a main amplifier and then to a discriminator to reject pulses from alpha particles. The discriminator output pulses were then taken to a 4096 channel magnetic tape time-of-flight analyser(7).

2.2 Fission Fragment Detectors

The small quantity of Pu^{241} available at the time of the experiment led to the choice of silicon-gold surface barrier semiconductor detectors as fission fragment detectors. These had the essential properties of speed, to counteract pile up(10) of pulses from alpha particles, and insensitivity to the intense burst of gamma radiation from the pulsed neutron source. They were prepared as described by Dearnaley and Whitehead(8) from 300 ohm-cm N-type silicon discs 1.8 cm diameter and 1 mm thick. The silicon was etched in a mixture of nitric, hydrofluoric and acetic acids (CP4) and mounted on a mica support with Araldite epoxy resin. Thin layers of gold (80 $\mu gm/cm^2$) were evaporated on each side of the silicon discs. Electrical contacts to the gold were made by silver gilt galvanometer wires attached with silver paste (Johnson Matthey FSP36). Fig. 5 shows a surface barrier detector and its associated circuitry. The fission detector used at 15m comprised four co-planar surface barrier detectors (B) in a 12.7 cm. diameter cylindrical brass chamber and is shown in Fig.4. The Pu^{241} was deposited on four platinum dishes (C) mounted close to the detectors. Fig.3 shows the arrangement used at 5m. Both chambers were continuously pumped by a rotary pump through thick filter paper mounted in a Yorkshire coupling between two discs of wire gauze[9]. The neutron beam entered the chamber through an aluminium window 0.08 cm. thick and left through a brass window 0.16 cm thick.

2.3 Measurement of the fission yield, neutron spectrum and background

Table 1 gives the experimental details for the fission yield experiments performed at 5m and 15m. Before the fission foils were prepared the Pu^{241} was separated from its Am^{241} daughter product. After separation the chambers could be used for three months before the count rate due to the pile up of alpha particle pulses from the decay of Am^{241} became unacceptable. In each experiment the sides of the detectors were shielded from background neutrons by 0.025 cm sheets of cadmium. During the 15m experiment a layer of boron carbide 0.27 $gm.cm^{-2}$ thick was kept in the neutron beam to remove neutrons whose time-of-flight was greater than the interval between successive bursts. In both experiments the neutron spectrum was measured by using a BF_3 counter (type 5EB40/13). This counter was 5 cm long 1.3 cm in diameter and contained BF_3 (96% B^{10}) at 40 cm. Hg pressure. To prevent overloading the amplifier by the gamma flash from the neutron source the voltage on the counter was held below 1500V. For the experiment at 5m both the fission chamber and the BF_3 counter could be placed side by side in the neutron beam. The fission yield and the neutron spectrum were measured simultaneously and recorded on magnetic tape. The tape recorder was coded to indicate from which detector each signal came.

The background for both fission and spectrum measurements was determined by placing the resonant scatterers listed in table 1 in the neutron beam. Each sample was sufficiently thick to remove all neutrons at the resonance energy. Measurements with and without resonant scatterers were normalised to each other using three neutron monitors mounted near the source. The presence of the resonant scatterers causes a decrease in the background being measured. The magnitude of this effect was determined by placing a second layer of resonant scatterer in the beam and finding the effective 'transmission' of the samples to the background neutrons. Figs. 6 and 7 show the fission and neutron counts per time channel as functions of neutron energy for the 5m experiment together with the backgrounds for these measurements. For both detectors the background may be represented by the equation

$$B = B_o + B_1 \exp(B_2 E) \qquad \ldots\ldots\ldots\ldots\ldots(1)$$

where B is the background counts per channel, E is the neutron energy and B_o, B_1 and B_2 are constants. These constants were determined by a least squares analysis. No background measurement is available below 0.178 eV. The data have therefore been evaluated on the basis of two possible assumptions. First, that the background below 0.178 eV is constant and equal to the value at 0.178 eV and second that a lower limit to the background below 0.01 eV is given by the count rate observed with the single layer of cadmium in the beam. The value of the fission cross section from 4 eV to 16 eV relative to the thermal value differs by 4% between these two assumptions. To compute the fission cross section from the 5m data a value of B_o equal to the mean of the two values in the above assumptions was taken which should not lead to more than 2% error due to background uncertainties. This has been included in the error estimated for the normalisation constant.

2.4 Calculation of the fission cross section and normalisation to the thermal fission cross section

The fission cross section (σ_f) for each timing channel (n) was calculated on an IBM-7030 computer from the equation

$$\sigma_f(E) = G\varepsilon(n')t(n')(A(n) - B(n))/(C(n') - D(n')) \qquad \ldots\ldots\ldots\ldots(2)$$

Here G is a normalisation constant, E is the neutron energy, t(n') is the neutron time-of-flight to channel n', A(n) the fission counts in channel n, C(n') the neutron counts in channel n', B(n) and D(n') are the fission and background counts per channel given by equation (1), and ε(n') is the calculated effect of self shielding on the BF_3 counter efficiency. The programme enables σ_f to be computed for unequal values of the fission and neutron detector flight path lengths. The neutron energy E is calculated at the centre of channel n and n' is the number of the channel containing E in the neutron spectrum experiment. A and C and the data used to determine the constants giving B and D were corrected for the 'dead time' arising in the time-of-flight analyser from the fact that the time for only one detected event could be recorded for each neutron burst. Equation (2) assumes that the $B^{10}(n\alpha)Li^{7}$ cross section used to measure the spectrum is proportional to $E^{-\frac{1}{2}}$. As well as the fission cross section the computer programme also calculates the neutron energy, the error in the fission cross section arising from statistical errors in A and C and constant fractional errors in B and D, the mean value of the cross section over energy ranges E to 2E and over the ranges E to 1.5E (beginning in each case from a value of E which must be chosen), the statistical error in these mean values and finally the contribution of each energy range to the resonance integral

$$\left(\int_{E}^{2E} \sigma_f \, \Delta E/E\right).$$

The normalisation constant G was determined for the 5m data by equating the value of the cross section at 0.0253 eV to 1010b[11]. Because of the low statistical accuracy of the data near thermal neutron energy all the data from 0.02 eV to 0.05 eV were used in the normalisation by assuming that $\sigma_f \sqrt{E}$ is a linear function of E over this energy range. A least squares analysis of the data was used to obtain the equation of this line which is shown in Fig.9. In this way a value of G with a statistical accuracy of $\pm$ 5.4% was obtained. For the 15m data the normalisation constant was determined by equating the areas under the fission cross section curve from 4 eV to 8 eV, 8 eV to 16 eV and 16 eV to 32 eV to the areas under the 5m results. The three estimates of the normalisation constant agreed to $\pm$ 2% giving a resultant error in the value of G for 15m of $\pm$ 5.6%. This error combined with the systematic uncertainty in G discussed in section 2.3 gives a final error in G of $\pm$ 6% for both sets of data.

3. Pu^{241} FISSION CROSS SECTION

3.1 The accuracy of the average cross section

Fig.8 shows the Pu^{241} fission cross section from 0.01 eV to 3 keV. In calculating the reactivity of a nuclear reactor an important consideration is the accuracy of the cross section data over wide energy bands. Table 2 lists the contributions to the error in the mean value of the fission cross section over energy ranges which are either E to 2E or E to 1.5E. The total error is a combination of the statistical error in the data, the error in the energy range due to the finite width of the timing channels and the errors in the normalising constants. Below 300 eV, except in the region of low cross section near 1 eV, the error in the mean value of the cross section over the range E to 2E is dominated by the error in the normalisation constant. Above this energy errors in the energy range become dominant.

3.2 Comparison with other data and with the multilevel curve of Simpson and Moore

It has long been noted that the shapes of resonances in the total and fission cross sections of fissile nuclei (U^{233}, U^{235}, Pu^{239} and Pu^{241}) are asymmetric and deviate from the single level Breit-Wigner shape[12,13,14]. These asymmetries have been attributed to multilevel interference due to the small number of fission channels available for the reaction. Simpson and Moore[1] have deduced multilevel parameters for Pu^{241} up to 11 eV by an analysis of the total cross section using the formulae of Reich and Moore[15]. A constant value of the radiation width ($\Gamma\gamma$) was assumed and it was found that the data were well described using a single spin state and two fission channels with the fission width of each resonance entirely in one or other of the channels. Simpson and Moore suggested that a more reasonable interpretation is that the resonances belong to two spin states each with one fission channel.

The parameters of Simpson and Moore have been used in the multilevel programme of Pattenden and Harvey[16], which is based on the formulae of Vogt[17], to determine the multilevel fission cross section. The programme calculates the Döppler and resolution broadened cross section.

Fig.9 shows $\sigma_f \sqrt{E}$ from 0.0087 eV to 0.12 eV, the multilevel cross section and the mean cross section given by Hughes and Schwarz[18]. The data agree well with the multilevel cross section over this energy range. Fig.10 shows that the data from 0.1 eV to 0.8 eV are in good agreement with the multilevel curve and also with the data of Leonard and Friesenhahn[13] renormalised to a thermal fission cross section of 1010b. However, there is substantial difference between the data and the mean curve given by Hughes and Schwartz near the 0.26 eV resonance.

Figs.11 and 12 show the 5m data and 15m data respectively over the energy range 3.5 eV to 11 eV and also the multilevel curve from the parameters of Simpson and Moore[1]. Except in the region of strong destructive interference near 4.8 eV the multilevel curve is in fair agreement with the data. These results confirm the conclusion of Watanabe and Simpson[2] that the assumptions made in the total cross section analysis of Pu^{241} by Simpson and Moore are substantially correct. It is significant however that the fission cross section measurements of Watanabe and Simpson between 3.5 eV and 11 eV deviate from the theoretical curve in the same way as the present data, being above the curve near 4.8 eV and below the curve at the peaks of the narrow resonances at 4.28 eV, 6.94 eV and 8.6 eV and also on the high energy side of the resonance at 10.2 eV. Brissenden and Durston[20] have shown that the disagreement in regions of strong interference, in particular near 4.8 eV, could be due to the approximations made in inverting the level matrix.

Recently Moore et al[22] have revised the multilevel parameters of Simpson and Moore to bring them into agreement with the total cross section data of Pattenden[23] and Craig and Westcott[24] which are thought to be more accurate than the data of Simpson and Schuman[25] near the peaks of the narrow resonances. The multilevel cross section given by the parameters of Moore et al[22] is shown as a dashed line in Fig. 12.

3.3 Multilevel analysis of data from 11 eV to 17 eV

A multilevel analysis of the data from 11 eV to 17 eV has been carried out in the following way:-

(1) Each resonance was analysed by the method of Lynn and Rae[21] to find $g\Gamma_n\Gamma_f$ and Γ from the single level Breit-Wigner formula corrected for Döppler and resolution broadening. Here Γ_n is the neutron width, Γ_f the fission width, Γ the total width of a resonance and g is the spin weighting factor.

(2) Γ_n and Γ_f were found by assuming a value of 0.040 eV for the radiation width $\Gamma\gamma$ and $g = 0.5$.

(3) These parameters were used in the multilevel programme of Pattenden and Harvey to give a Döppler and resolution broadened multilevel curve. The effective temperature used to calculate the Döppler width was $307^{o}K$[27]. It was assumed that all resonances are in one spin state and that there are two fission channels. The fission width of each level was assumed to lie entirely in one of the two channels. The choice of channel and the relative sign of the vector component $(\Gamma_f/2)^{\frac{1}{2}}$ for each level was guided by the value of the cross section between two levels.

(4) The resultant curve was compared with the data.

(5) The level parameters, the choice of channel and the relative signs of $(\Gamma_f/2)^{\frac{1}{2}}$ were modified and steps (3), (4) and (5) repeated until the curve shown in Fig.13, which is derived from the parameters given in Table 3, was obtained. Because the fit is not unique no errors can be assigned to these multilevel parameters. These parameters, the grouping of levels into channels and the relative sign of $(\Gamma_{f_i}/2)^{\frac{1}{2}}$ are in fair agreement with multilevel parameters deduced recently by Moore et al[22]. with the exception that these authors do not see a level at 14.04 eV. The following conclusions on the choice of channel for each level emerged from the multilevel analysis.

(i) Full interference was required between the levels at 14.04 eV, 16.06 eV and 14.78 eV to explain the high cross section between these levels.

(ii) The cross section between 16.06 eV and 16.7 eV required that these two levels do not interfere.

(iii) Similarly the level at 13.45 eV could not interfere with its neighbouring resonances at 12.84 eV and 14.04 eV.

3.4 The average resonance parameters

Fig.14 shows the number of resonances observed below an energy E as a function of E. This figure indicates that resonances begin to be missed at about 20 eV. Below this energy the mean level spacing D is 1.3 ± 0.2 eV. This value, combined with the data of Simpson and Moore and the data from Table 3 gives a strength function, $\overline{g\Gamma_n^0}/D$, of $(1.4 \pm 0.6).10^{-4}$. Fig.15 shows the number of resonances with a value of $\Gamma_f/\overline{\Gamma_f}$ below that given on the abscissa, where Γ_f is the fission width and $\overline{\Gamma_f}$ the mean fission width for all levels. An analysis of this histogram by the maximum likelihood method[26)] shows that it fits a chi-squared distribution with a number of degrees of freedom $\nu = 2 \pm 0.2$. It is known that the resonances belong to two spin states which may have widely different values of $\overline{\Gamma_f}$, the value of ν for the combined distribution is not therefore meaningful. Although in principle the multilevel analysis leads to a separation of the resonances into two groups which can be assumed to correspond to the two spin states, the large energy gap between the two levels at 10.2 eV and 12.8 eV prevents the manifestation of any interference effects between these two levels. It is not possible to say therefore which of the fission channels above 11 eV corresponds to one of the channels below 11 eV and the value of ν for the distribution of $\Gamma_f/\overline{\Gamma_f}$ for resonances belonging to one channel cannot be given. No arbitrary combination of the channels found below 11 eV with the channels above 11 eV leads to a value of ν less than 2. The resonances from 11 eV to 17 eV do not fall into distinctly 'broad' and 'narrow' groups characteristic of the levels below 11 eV. From 11 eV to 17 eV the mean values of the fission widths for the two channels are 0.236 eV and 0.111 eV in contrast to the mean values below 11 eV 0.85 eV and 0.074 eV.

4. CONCLUSION

The measurement of the fission cross section of Pu^{241} which has been carried out from 0.0087 eV to 3 keV gives the mean value of the cross section over energy ranges E to 2E to ± 7% below 250 eV except in a region of low cross section near 1 eV. At energies above 250 eV the major contribution to the error in the mean value of the cross section comes from the error in the energy range due to the finite timing channel width. From 0.1 eV to 0.5 eV the data agree in shape with those of Leonard and Friesenhahn to ± 5%. Up to 11 eV the data are in fair agreement with the multilevel curve of Simpson and Moore and confirm that the assumptions made in this anaysis are substantially correct. It is noticeable, however, that the deviations from this curve are similar to the deviations exhibited by the data of Watanabe and Simpson. At the peaks of the narrow resonances the data agree well with the multilevel curve of Moore et al[22]. The multilevel anaysis of the data has been extended from 11 eV to 17 eV, this leads to a strength function of $(1.4 \pm 0.6)10^{-4}$ based on a mean level spacing of 1.3 ± 0.2 eV. Over this energy range most of the parameters are in fair agreement with those of Moore et al[22]. Improvements in the data would require greater statistical accuracy at low energy to reduce the error in the normalisation constant and better energy resolution to reduce the error in the energy ranges at high energy. Both these could be accomplished using more fissile material in the fission chamber. This would best be done using a gas scintillator fission fragment detector which would reduce the pile-up of alpha pulses from the Am^{241} daughter product and enable the detector to be used for a longer time.

ACKNOWLEDGEMENTS

The author is grateful to Dr. M. J. Poole and Dr. E. R. Rae for their advice and encouragement, to Mr. R. W. McIlroy and Mr. D. Boreham for separating the Pu^{241} from its product Am^{241}, preparing the foils and loading them into the fission chambers and to Mr. D. A. J. Endacott for assistance with the experiment.

REFERENCES

1. SIMPSON, O.D., and MOORE, M.S., Phys. Rev. 123, 559 (1961).
2. WATANABE, T., and SIMPSON, O.D., Phys. Rev. 133, B390 (1964).
3. LEONARD, B.R., and FRIESENHAHN, S.J., HW-62727, unpublished.
4. RICHMOND, R., and PRICE, B.T., J. Nuclear Energy 2, 177 (1956).
5. ADAMCHUK, GERASIMOV, YEFIMOV, ZENKEVICH, MOSTOVOI, PEVZNER, CHERNYSHOV and TSITOVICH, Proc. Int. Conf. on peaceful uses of atomic energy, UN, New York, 1956, vol.4, paper 645.
6. POOLE, M.J., and WIBLIN, E.R., Second United Nations Int. Conf. on the peaceful uses of atomic energy, vol.14 (United Nations, Geneva, 1958) p.226.
7. WATERS, J.R., and BIRD, J.R., Nucleonics 19 (1961) 70.
8. DEARNALEY, G., and WHITEHEAD, A.B., Nuclear Instr. and Methods, 12, 205, (1961).
9. EVANS, J.P., and LEE, J.A., Report AERE-M/M214, unpublished.
10. ROSSI, B.B., and STAUB, H.H., Ionisation chambers and counters (McGraw-Hill Publ. Co., New York, 1949).
11. HUGHES, D.J., MAGURNO, B.A., and BRUSSEL, M.K., Supplement 1 to BNL 325 (2nd Ed.).
12. SHORE, F.J., and SAILOR, V.L., Phys. Rev. 112, 191, (1958).
13. MOORE, M.S., and REICH, C.W., Phys. Rev. 118, 718 (1960).
14. BOLLINGER, L.M., COTE, R.E, and THOMAS, G.E., Second United Nations Int. Conf. on the peaceful uses of atomic energy, United Nations, Geneva, vol.15, 127 (1958).
15. REICH, C.W., and MOORE, M.S., Phys. Rev. 111, 929 (1958).
16. PATTENDEN, N.J., and HARVEY, J.A., Proc. Int. Conf. on nuclear structure (North-Holland Publ. Co., Amsterdam, 1960). p.882.
17. VOGT, E., Phys. Rev. 112, 203 (1958).
18. HUGHES, D.J., and SCHWARTZ, R.B., BNL-325 (2nd Ed.).
19. HUGHES, D.J., MAGURNO, B.A., and BRUSSEL, M.K., Suppl. No.1 to BNL-325 (2nd Ed.).
20. BRISSENDEN, R.J., and DURSTON, C., private communication.
21. LYNN, J.E., and RAE, E.R., J. Nuc. En. 4 (1957) 418.
22. MOORE, M.S., SIMPSON, O.D., WATANABE, T., RUSSELL, J.E., and HOCKENBURY, R.W. - to be published.

23. PATTENDEN, N.J., and BARDSLEY, S., Proceedings of the International Conference on Neutron Physics with Reactor Neutrons, U.A.S.E.C. Report ANL-6797 p.369 (1963) (unpublished).

24. CRAIG, D.S., and WESTCOTT, C.H., Bull. Am. Phys. Soc. Ser.II, 7, 305 (1962).

25. SIMPSON, O.D., and SCHUMAN, R.P., Nuc. Sci. Eng. 11, 111 (1961).

26. PORTER, C.E., and THOMAS, R.G., Phys. Rev. 104, 483, (1956).

27. JACKSON, H.E., and LYNN, J.E., Phys. Rev. 127, 461, (1962) and J.E. Lynn (private communication).

TABLE 1

Experimental Details

	5m Experiment	15m Experiment
Weight of Pu^{241}	5 mg	10 mg
Superficial density	1 mg cm^{-2}	1 mg cm^{-2}
Number of detectors	2	4
Sensitive area of each detector	2 cm^2	2 cm^2
Isotopic content of material Pu^{239}	0.52%	2.5%
Pu^{240}	1.44%	2.48%
Pu^{241}	97.33%	94.8%
Pu^{242}	0.71%	0.28%
Neutron filter	None	0.27 gm cm^{-2} B_4C
Materials used to determine background	W 18.8 eV	Na 2.3 keV
('Black' samples)	Ta 4.28 eV	Mn 335 eV
	In 4.28 eV	Ta 4.28 eV
	Cd 0.178 eV	In 1.457 eV
Electron pulse width	1/5 μsec.	1 μsec.
Timing channel width	1 μsec.	1 μsec.
Pulse repetition frequency	110 pps	200 pps

TABLE 2

Accuracy of the mean fission cross section

Neutron energy E (eV)	Energy range a)	Statistical accuracy c)		Error in energy range c)		Error in G b)c)	Total error in mean cross section c)	
		5m data	15m data	5m data	15m data		5m data	15m data
0.01-0.05	E-1.5E	2		0.1		6	6.3	
0.05-0.3	E-1.5E	1.3		0.6		6	6.1	
0.3 -0.43	E-1.5E	2		0.6		6	6.3	
0.43-1	E-1.5E	8		0.6		6	10	
1 -2	E-2E	7		0.8		6	9	
2 -4	E-2E	5		1.2		6	8	
4 -8	E-2E	1.5	1.3	1.7	0.6	6	6.4	6.2
8 -16	E-2E	2	1.6	2.4	0.8	6	6.7	6.2
16- 32	E-2E	2.4	1.8	3	1.0	6	7.1	6.3
32-256	E-2E		2.3		<3.5	6		<7.3
256-3000	E-2E		2.6		<10	6		<12

a) Range of energy used to find mean value of σ_f

b) G is the normalisation constant

c) per-cent.

TABLE 3

Multilevel parameters for Pu^{241} between 12 eV and 17 eV

E_λ (eV)	$2g\Gamma_n^{\,o}$ (10^{-3} eV)	Γ_{f1} (10^{-3} eV)	Γ_{f2} (10^{-3} eV)	$\Gamma\gamma$ (10^{-3} eV)	Sign of $(\Gamma_{fi}/2)^{\frac{1}{2}}$
12.84	0.220	266		40	+
13.45	0.596		42	40	-
14.04	0.048	214		40	-
14.78	1.513	105		40	+
16.06	0.344	360		40	-
16.70	0.323		180	40	+

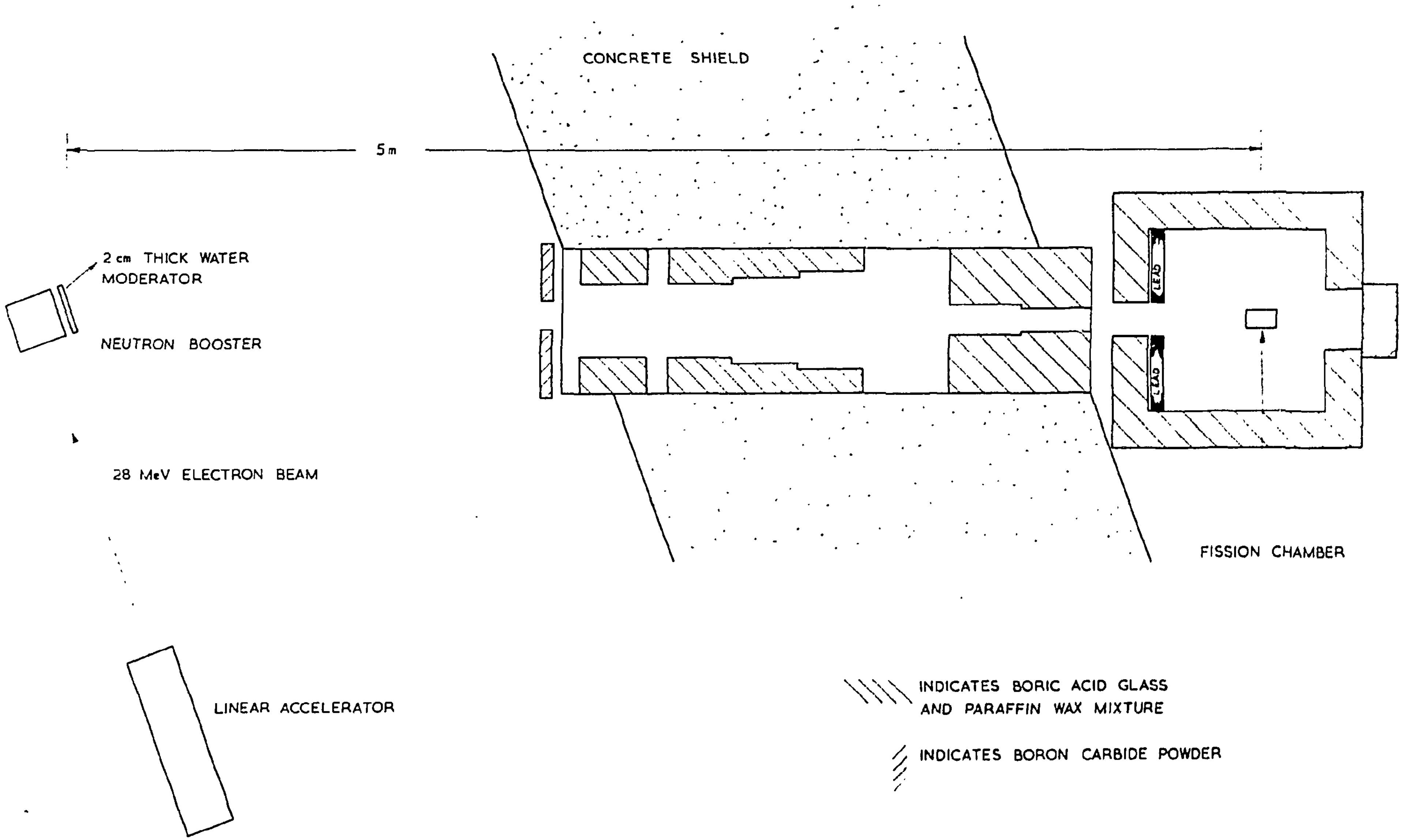

A.E.R.E. R 4597. FIG. 1. 5m FLIGHT PATH LAYOUT

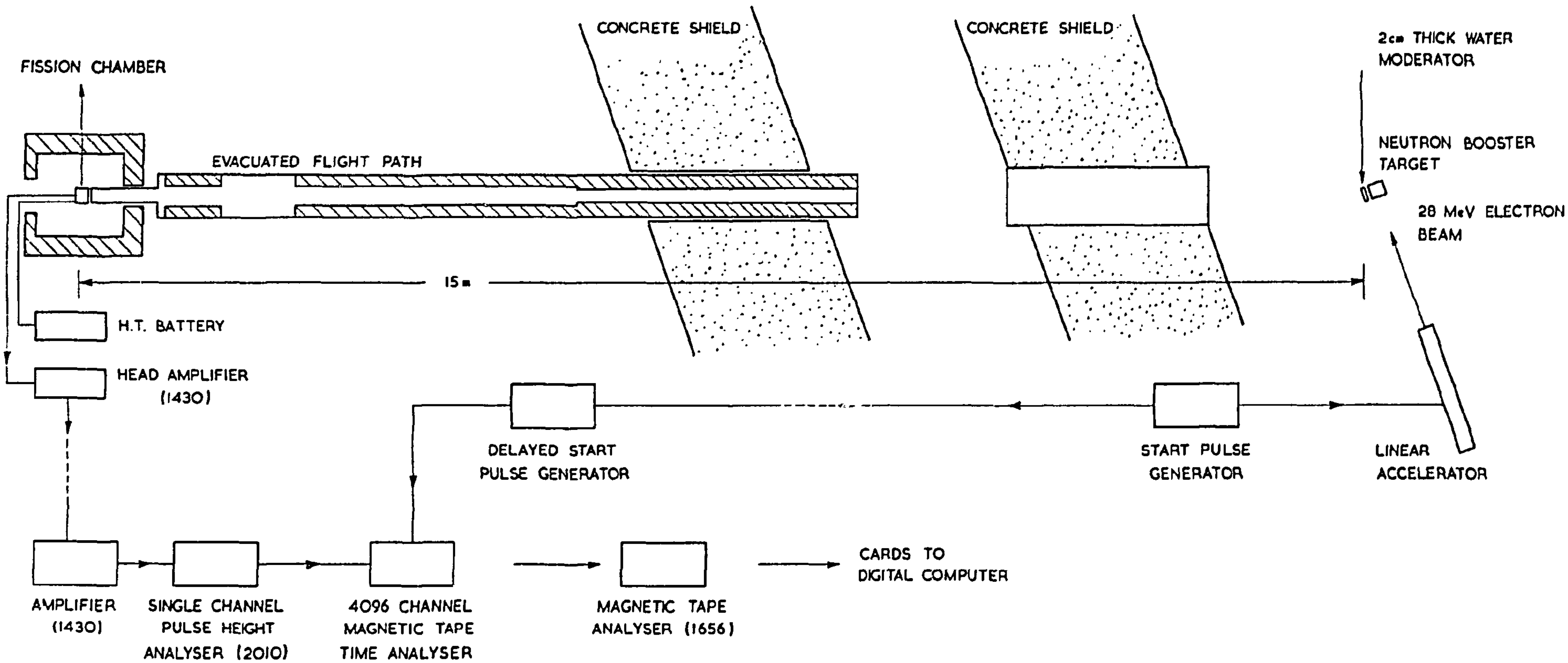

A.E.R.E. R4597. FIG. 2. 15m FLIGHT PATH LAYOUT AND SCHEMATIC DIAGRAM OF EQUIPMENT

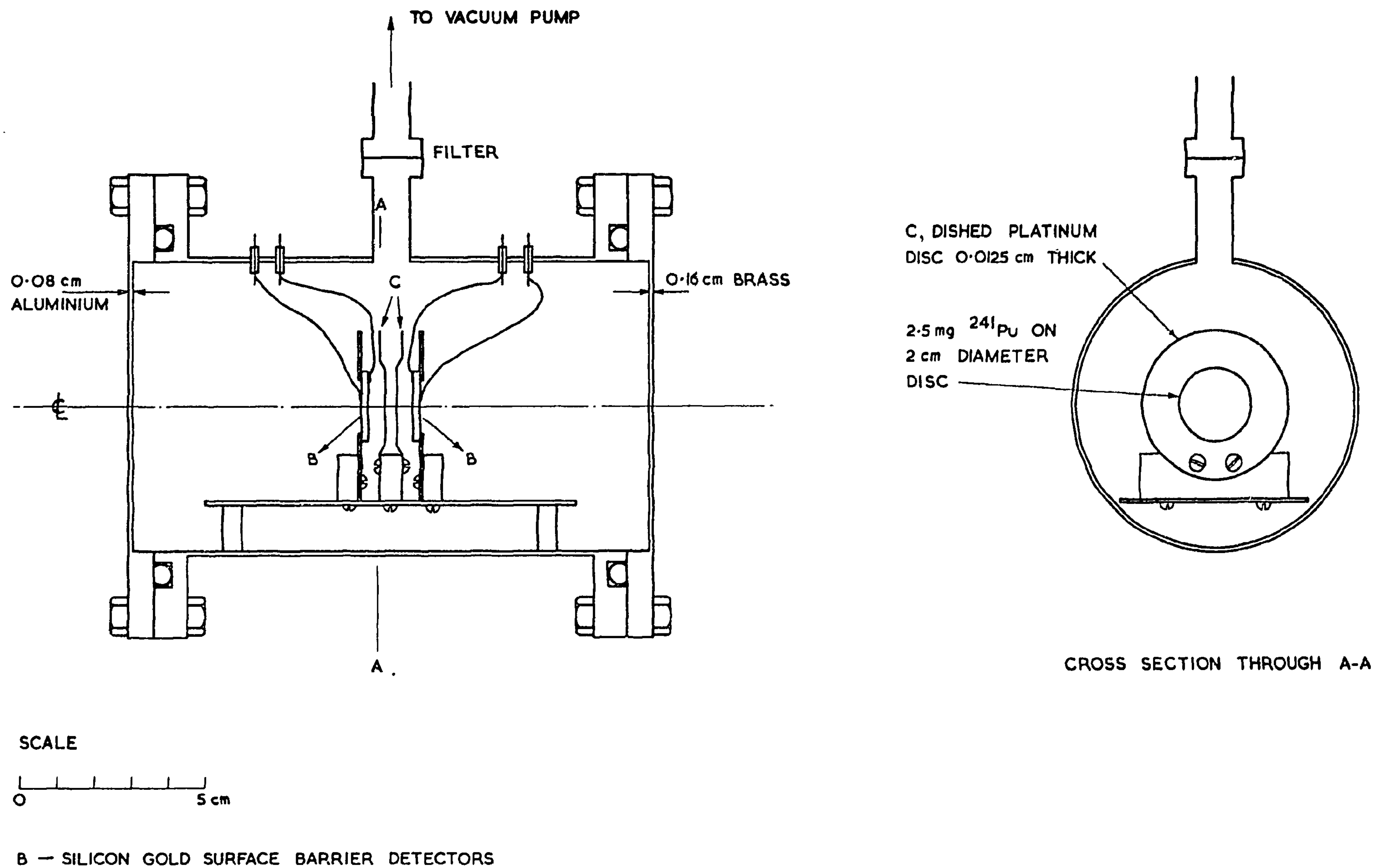

A.E.R.E. R 4597. FIG. 3. THE ^{241}Pu FISSION FRAGMENT USED AT 5m

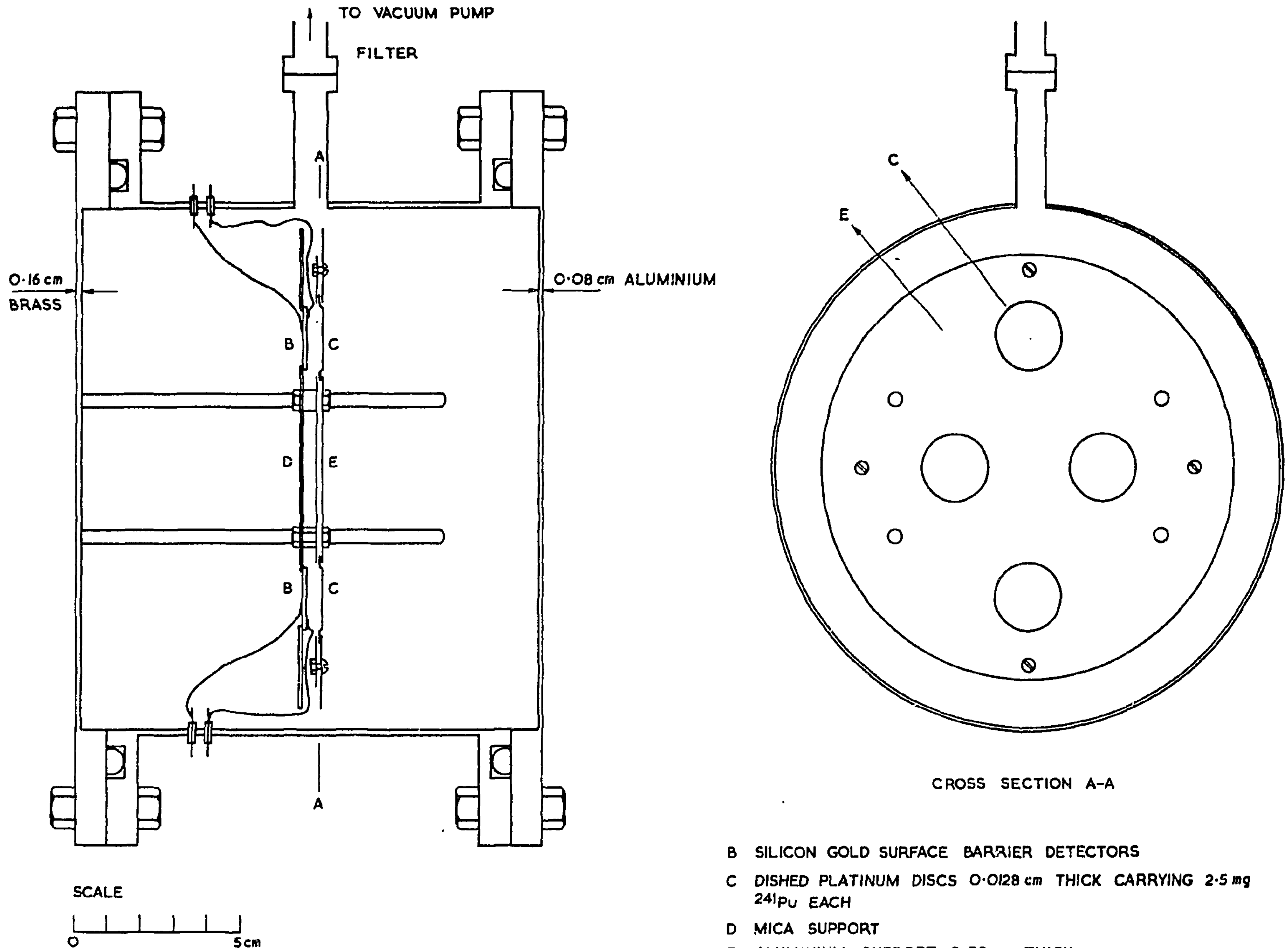

B SILICON GOLD SURFACE BARRIER DETECTORS

C DISHED PLATINUM DISCS 0·0128 cm THICK CARRYING 2·5 mg ^{241}Pu EACH

D MICA SUPPORT

E ALUMINIUM SUPPORT 0·08 cm THICK

A.E.R.E. R.4597. FIG. 4. THE ^{241}Pu FISSION FRAGMENT DETECTOR USED AT 15m

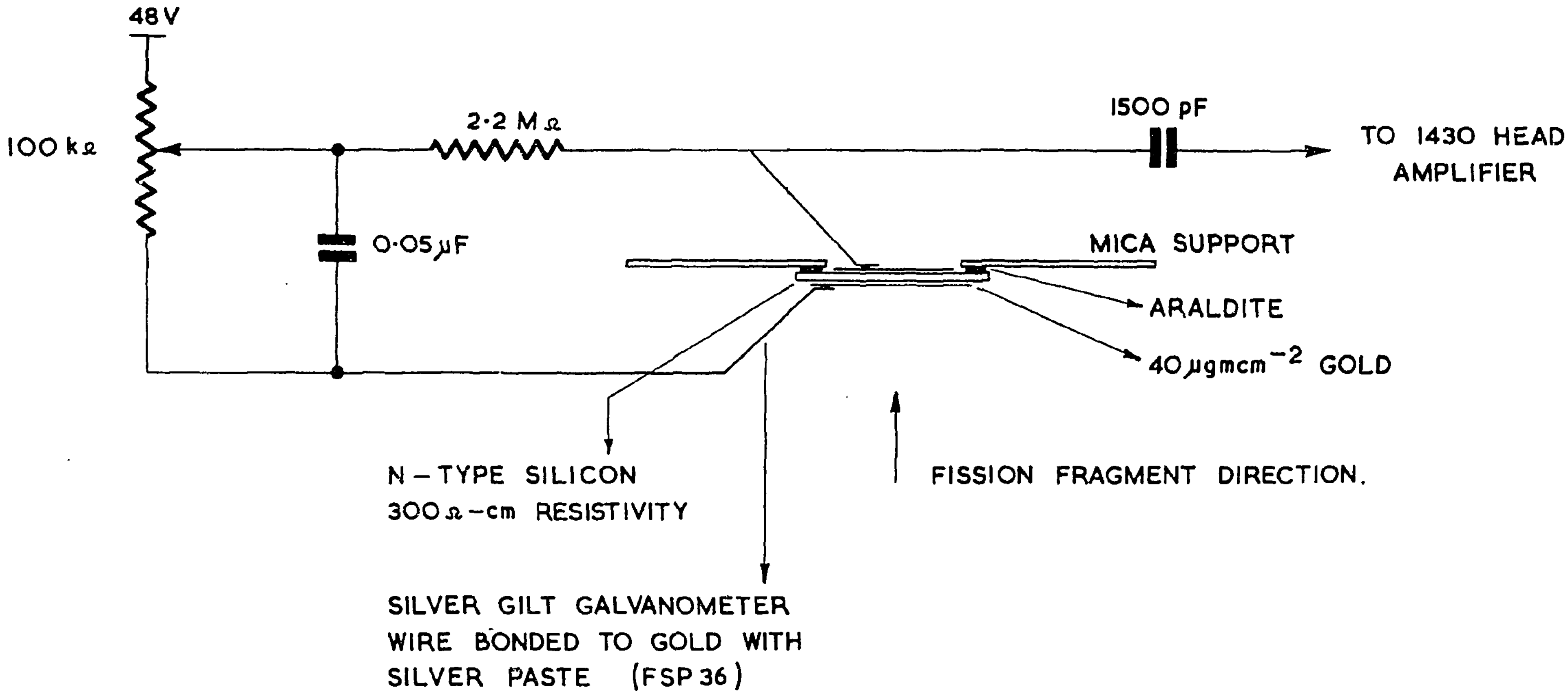

A.E.R.E. R 4597 FIG. 5. SILICON GOLD SURFACE BARRIER DETECTOR AND CIRCUIT

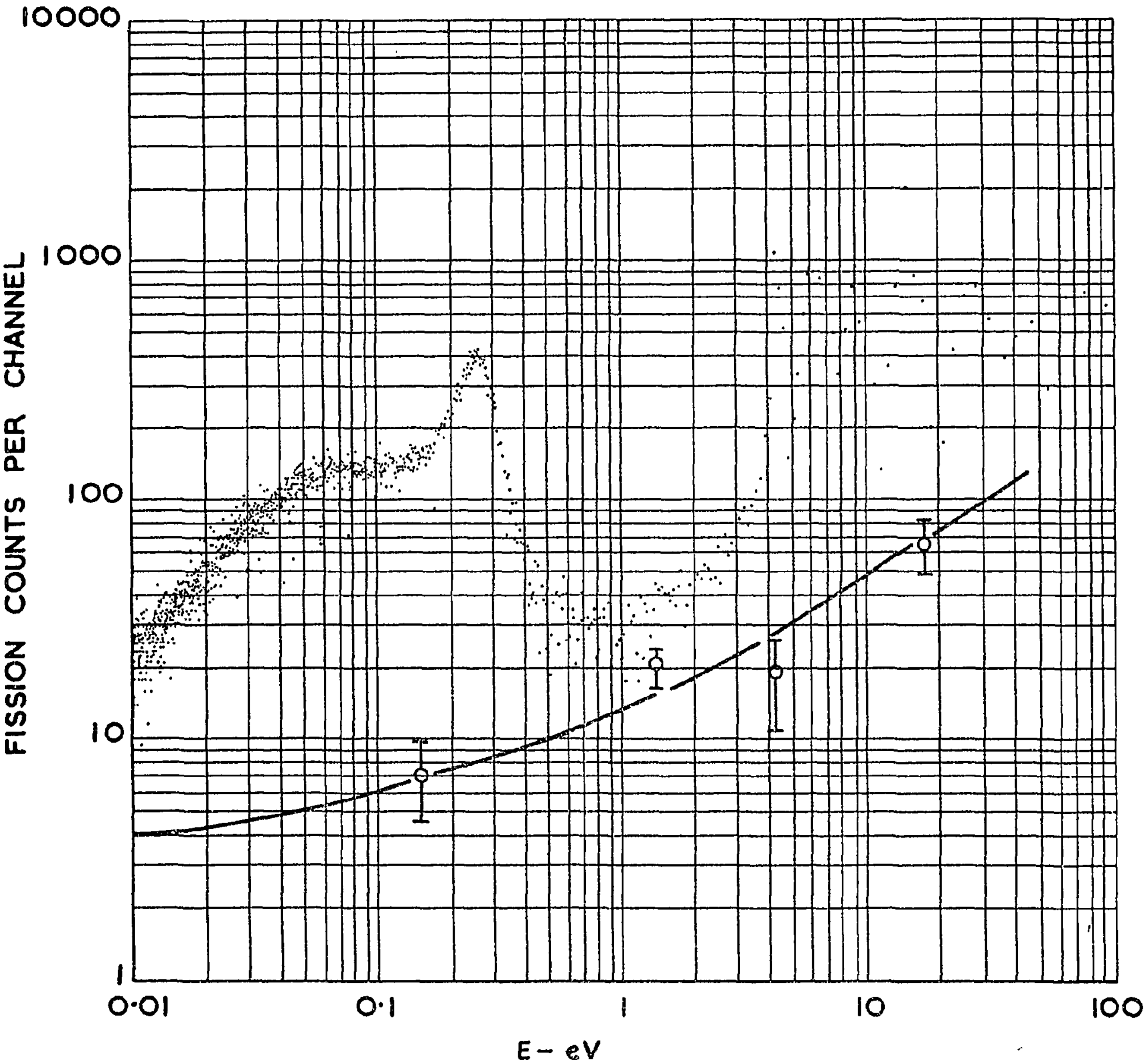

A.E.R.E. R.4597. FIG. 6. 5m FISSION COUNTS PER CHANNEL AND BACKGROUND (SOLID LINE)

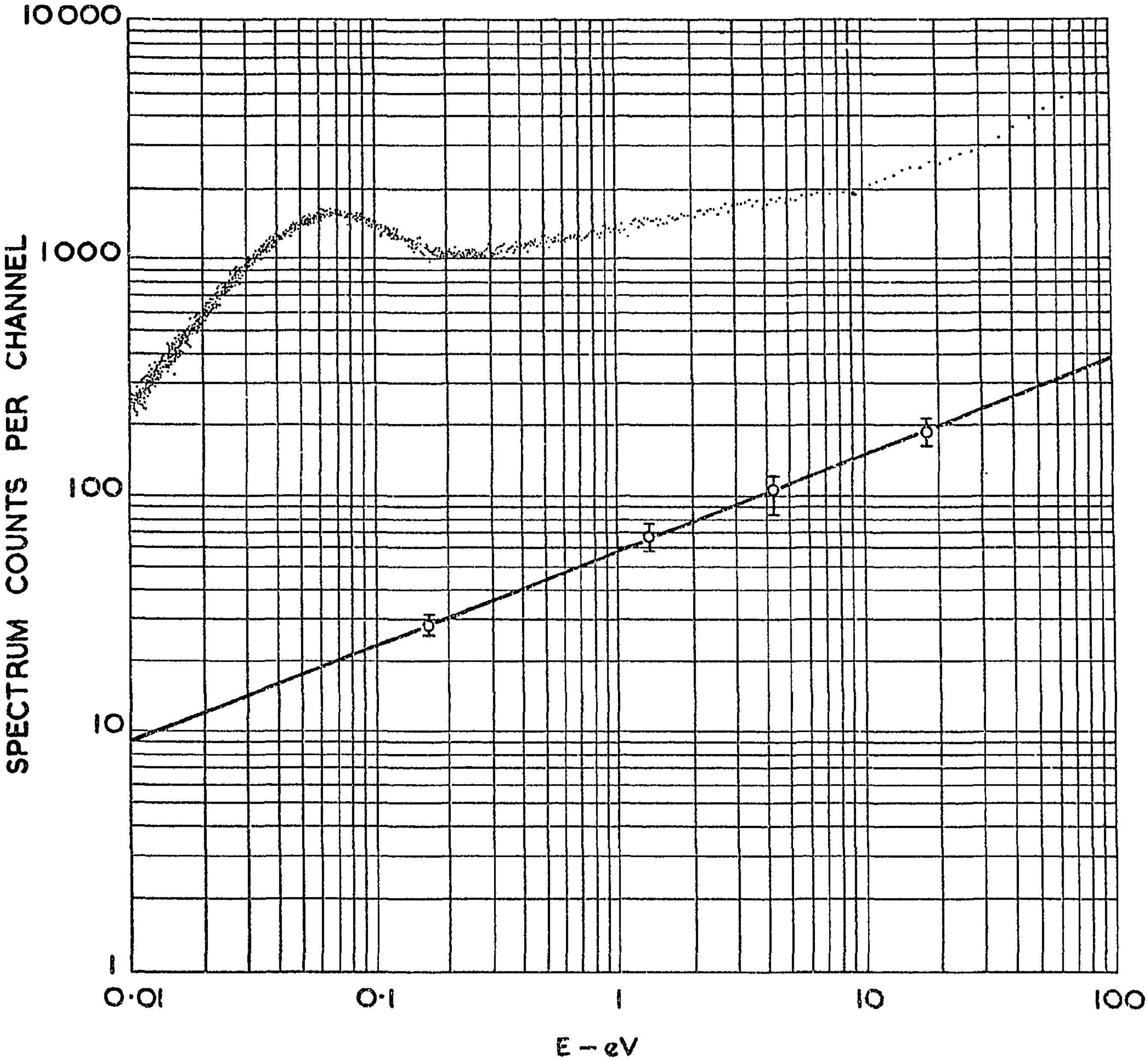

A.E.R.E. R.4597 FIG. 7. 5m NEUTRON SPECTRUM AND BACKGROUND (SOLID LINE)

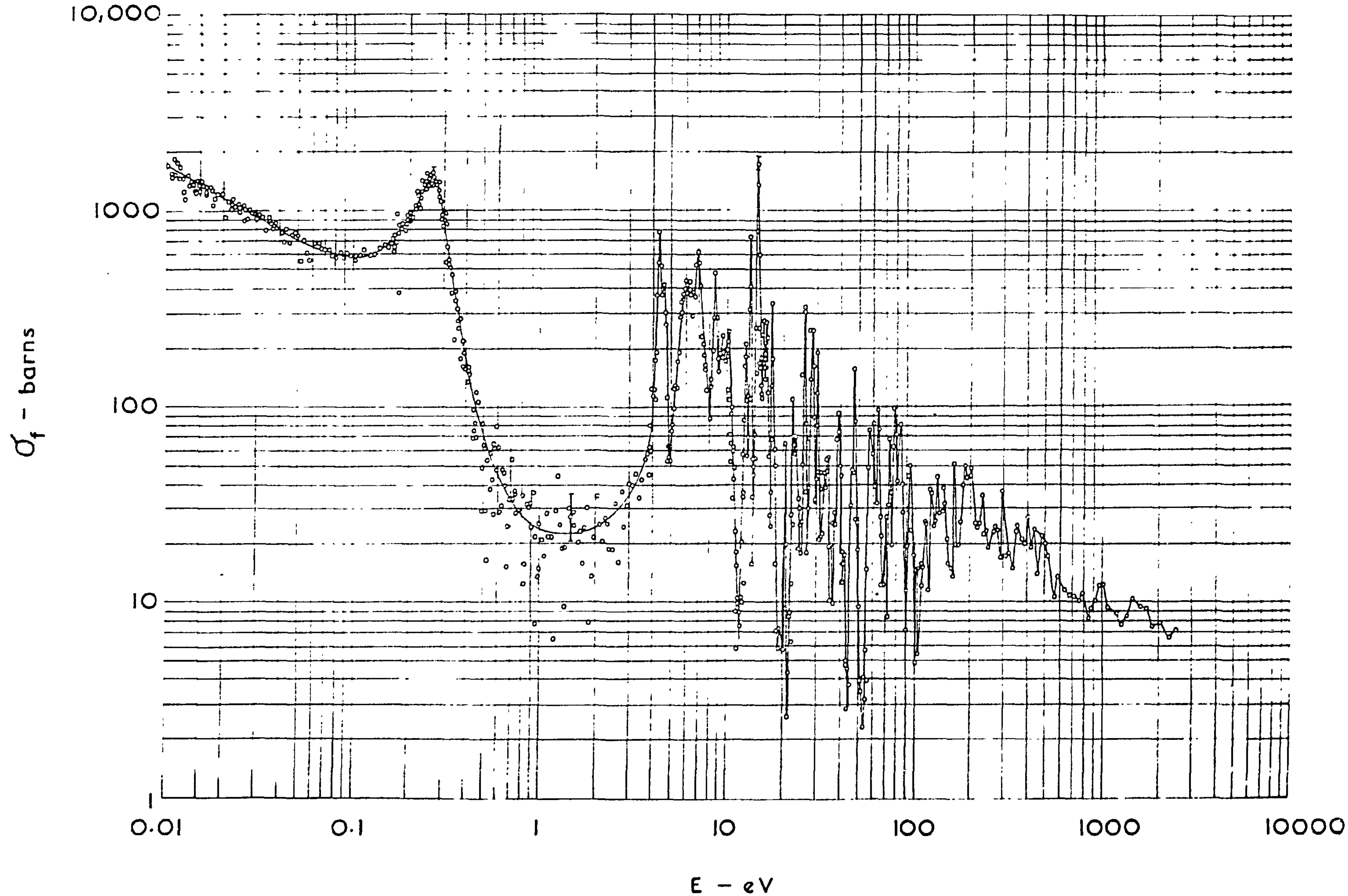

A.E.R.E. R.4597 FIG. 8. THE FISSION CROSS SECTION OF Pu^{241} FROM 0·01eV TO 3000eV.

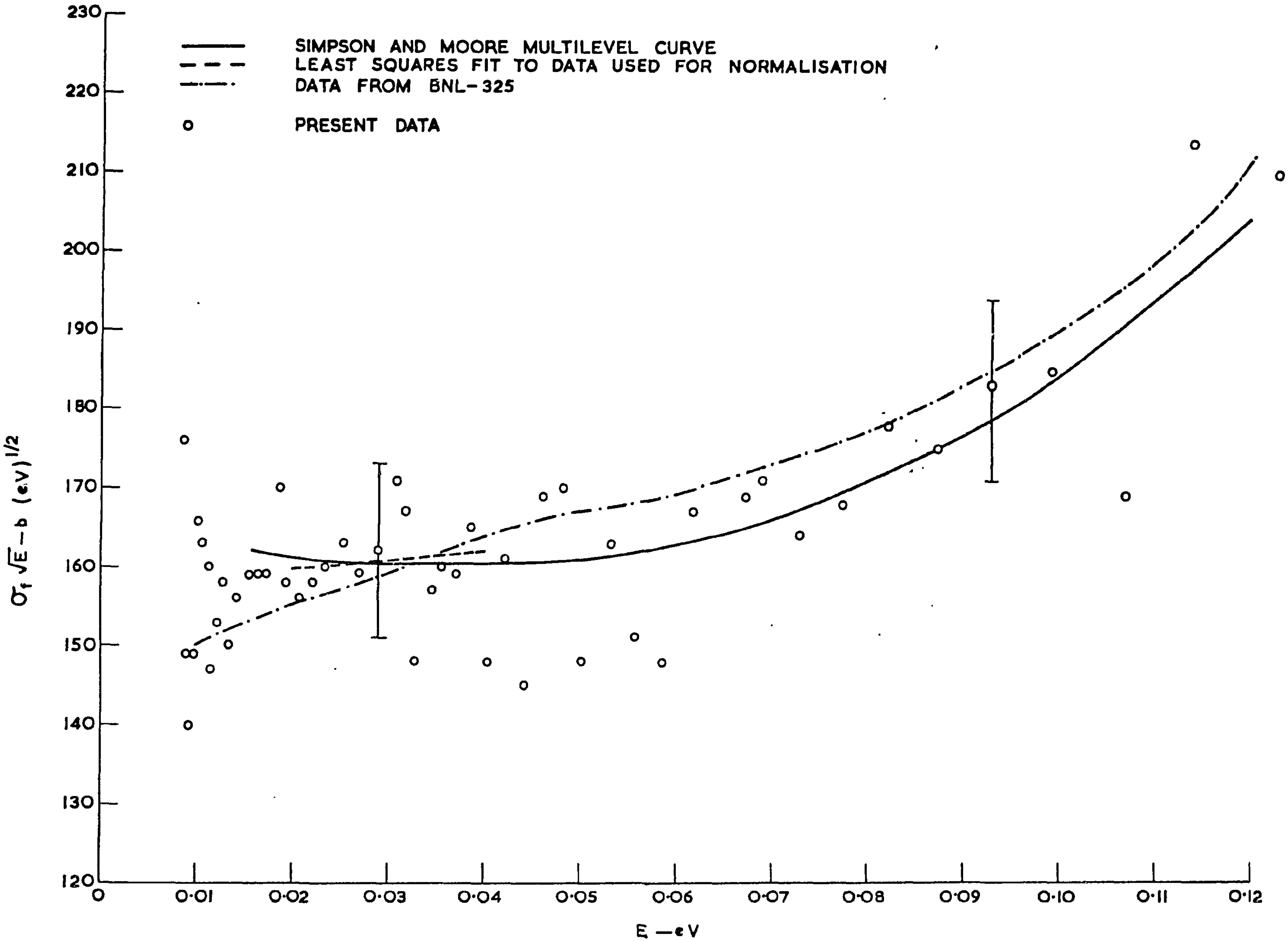

A.E.R.E. R.4597 FIG. 9. $\sigma_f \sqrt{E}$ FROM 0·0087eV TO 0·12eV.

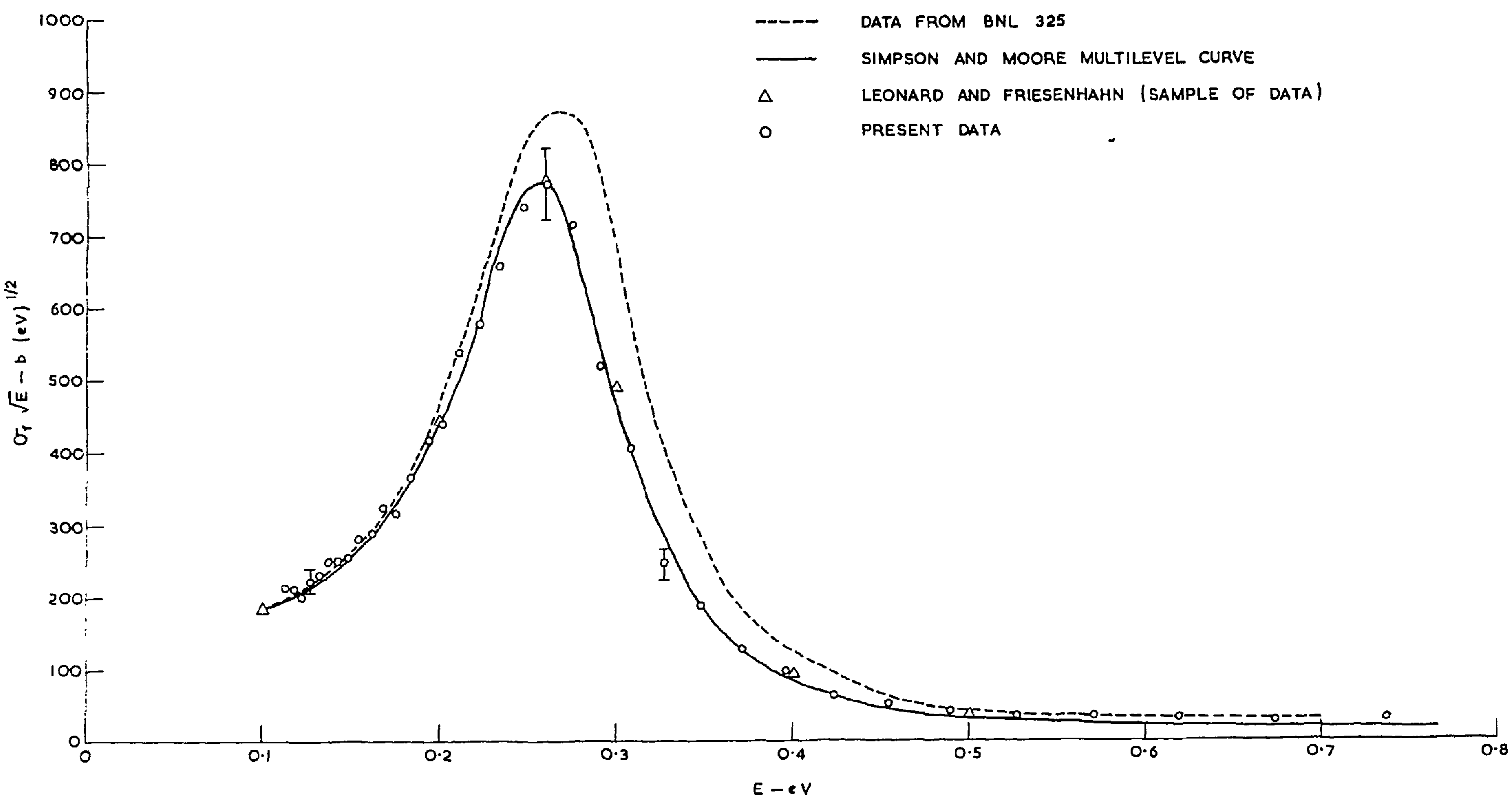

A.E.R.E. R.4597 FIG. 10. $\sigma_f \sqrt{E}$ FOR Pu–241

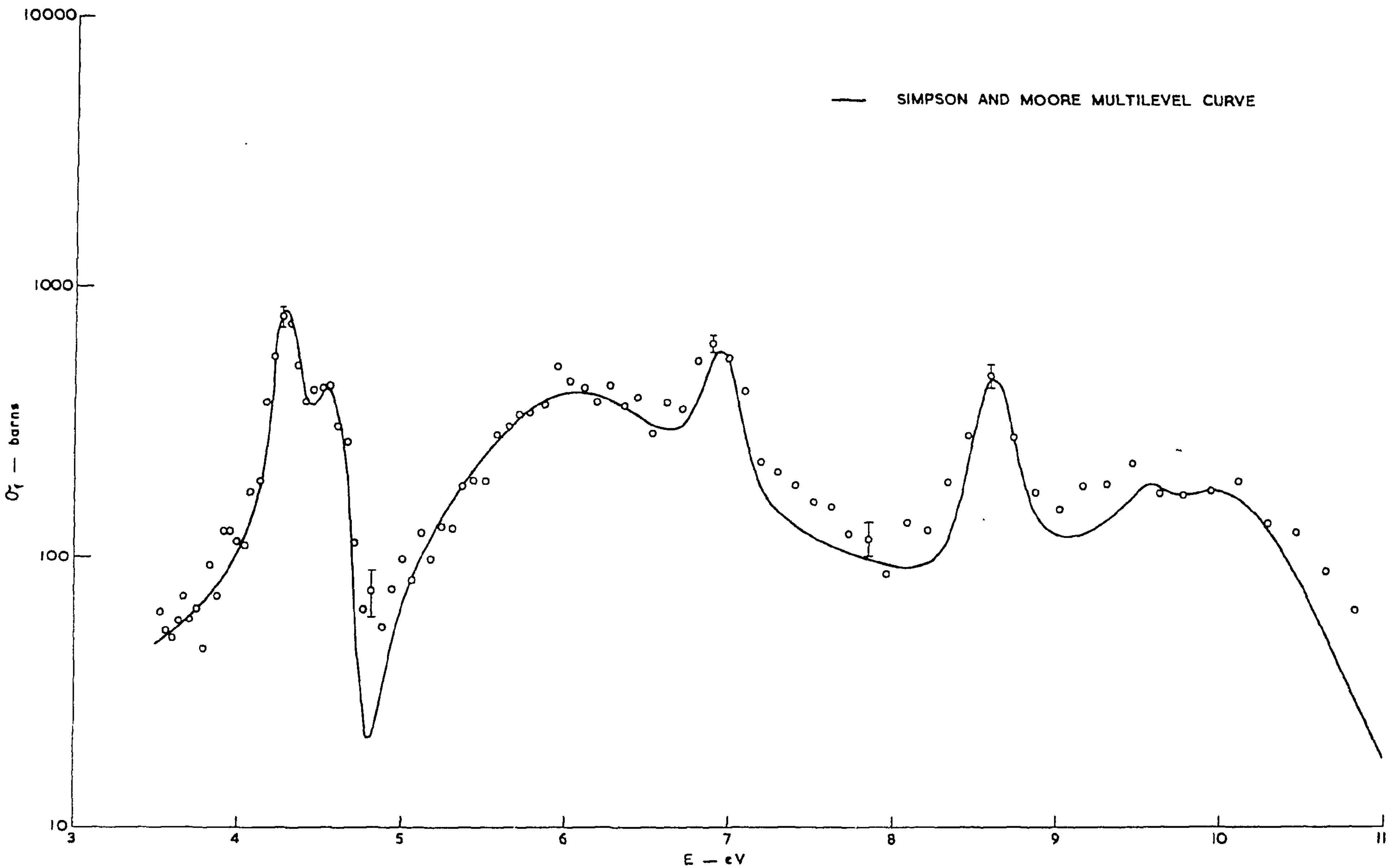

A.E.R.E. R 4597. FIG. 11. Pu^{241} FISSION CROSS SECTION FROM 3 eV TO 11 eV 5 m DATA

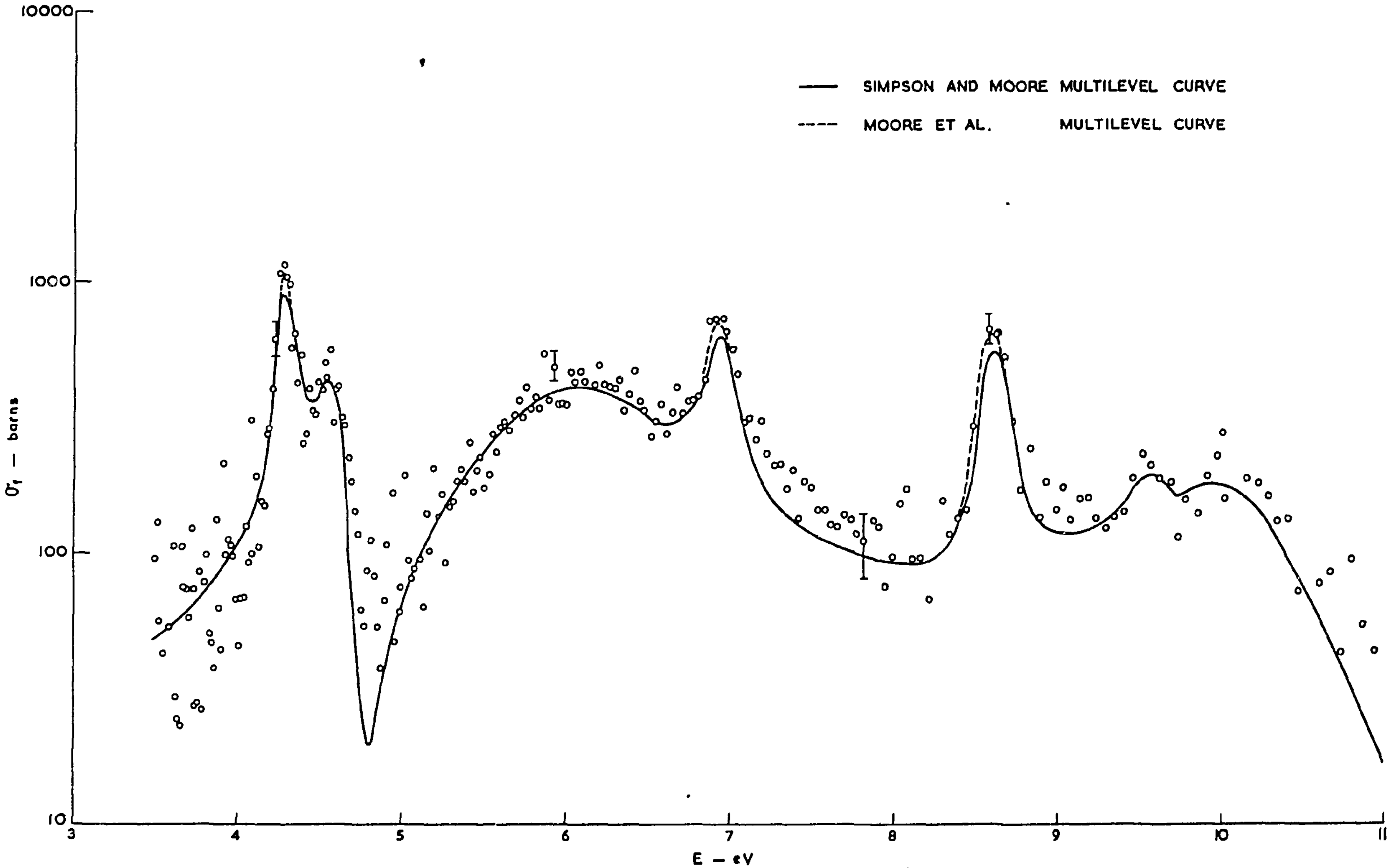

A.E.R.E. R 4597. FIG. 12. Pu^{241} FISSION CROSS SECTION FROM 3 eV TO 11 eV 15m DATA

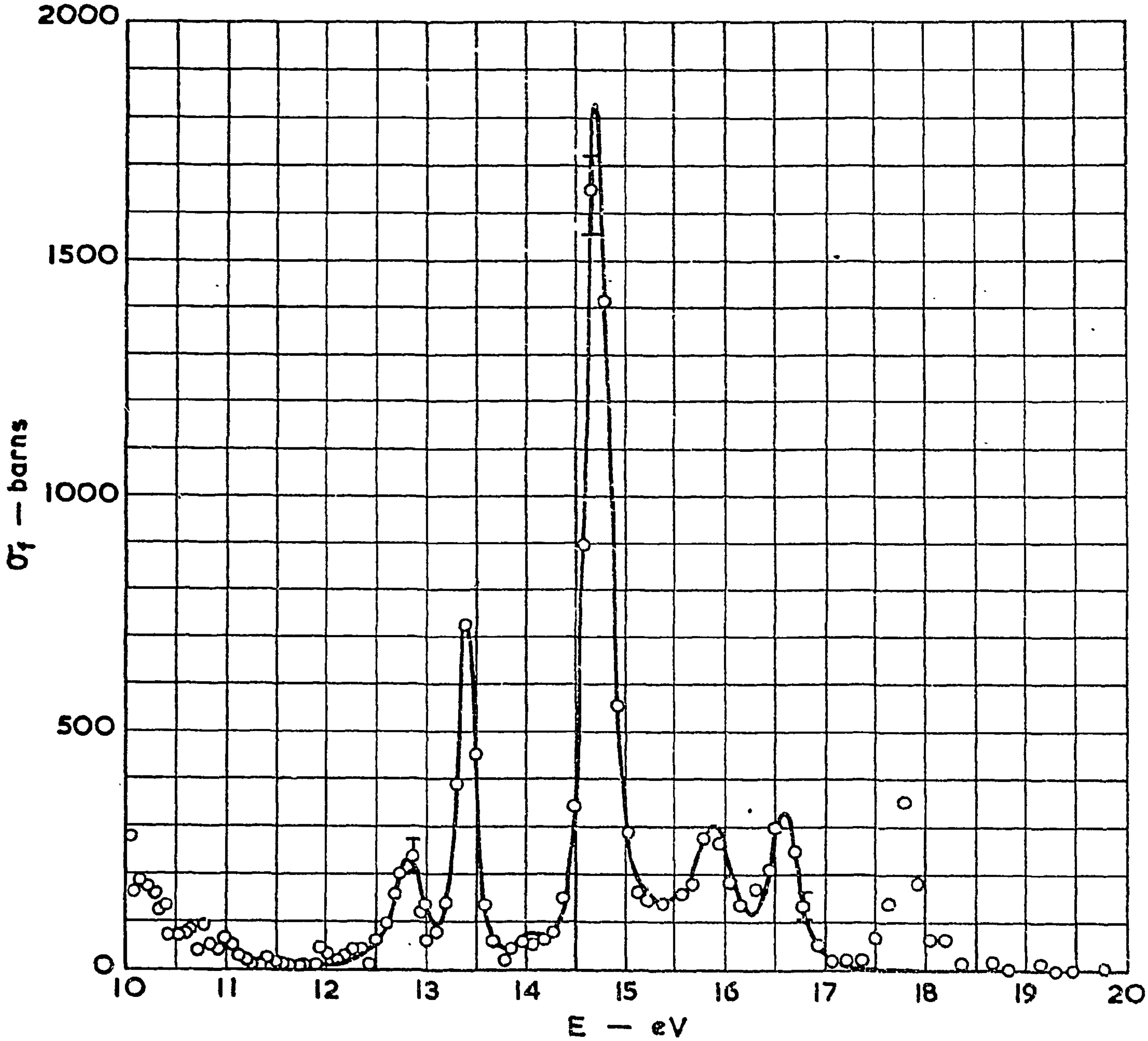

A.E.R.E. R 4597. FIG. 13. Pu^{241} FISSION CROSS SECTION FROM 10eV TO 20eV. SOLID LINE IS MULTILEVEL FIT OF TABLE 3.

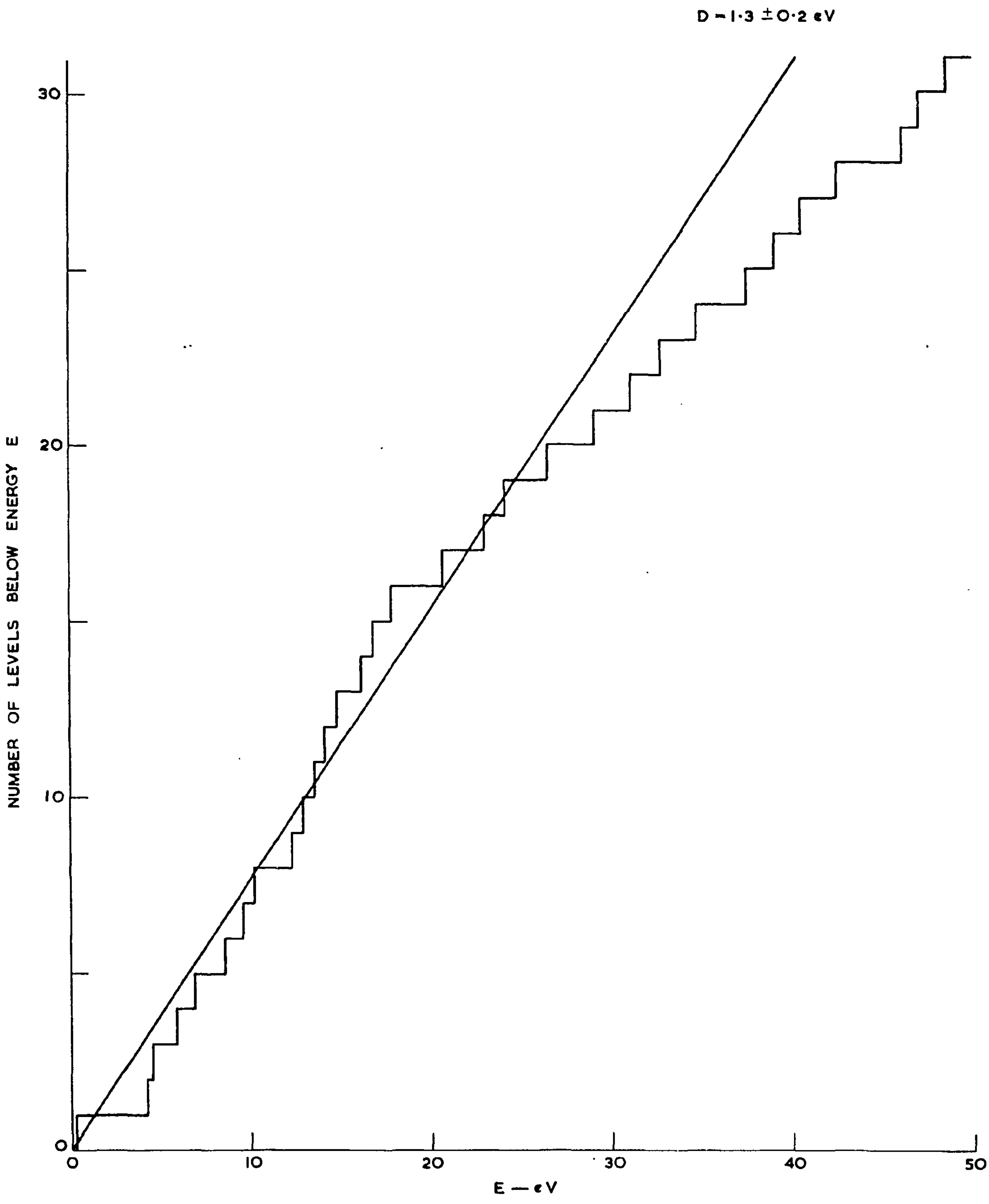

A.E.R.E. R 4597. FIG. 14. NUMBER OF LEVELS BELOW ENERGY E AS A FUNCTION OF E

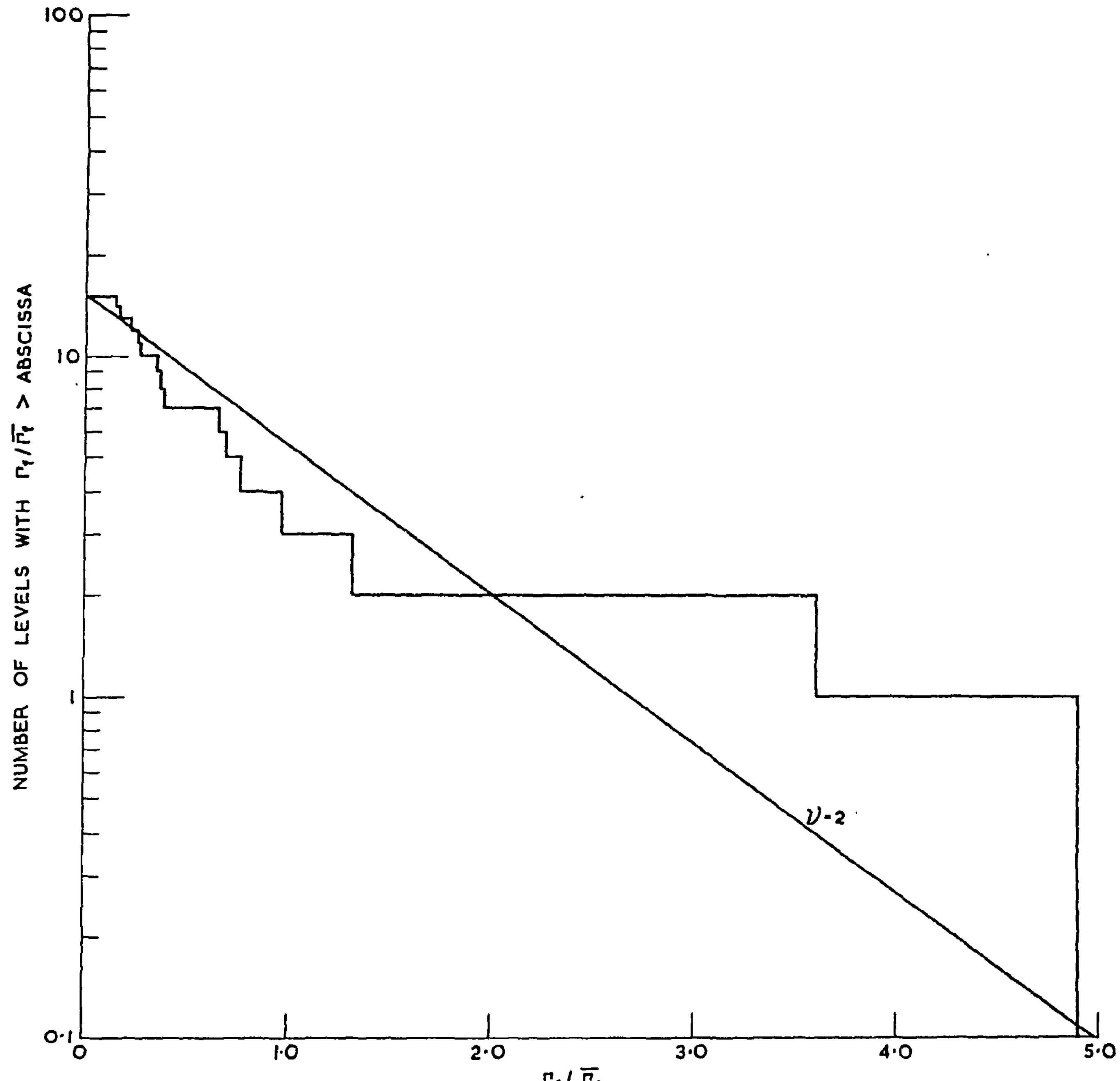

A.E.R.E. R 4597 FIG. 15. THE DISTRIBUTION OF $\Gamma_f / \bar{\Gamma}_f$